# Amorphous Cis-1,4-Polybutadiene P-V-T properties from atomistic simulations

**Aigul Shamsieva**
Kazan Federal University
**Irina Piyanzina**
Kazan Federal University
**Benoit Minisini** ( bminisini@materialsdesign.com )
Materials Design (France)

**Research Article**

**Keywords:** polybutadiene, glass transition temperature, pressure, molecular dynamic simulations

**Posted Date:** April 27th, 2023

**DOI:** https://doi.org/10.21203/rs.3.rs-2815978/v1



**Version of Record:** A version of this preprint was published at Journal of Molecular Modeling on July 14th, 2023. See the published version at https://doi.org/10.1007/s00894-023-05658-6.

# Abstract

### Context

The experimental values of variation of glass transition temperature (Tg) with the pressure are relatively dispersed due to the diversity of microstructure encountered in Cis-1,4-Polybutadiene (PB) and the diversity of technics used for its measurement. Fortunately, atomistic simulations allow to get valuable information for very well controlled chemistry and structures using very well-defined protocol of acquisition. That's why, atomistic modelling will be used to evaluate the variation of Tg with the pressure for a well-defined amorphous oligomer of cis-1,4 PB.

### Method

Atomistic dilatometry was performed on model of amorphous cis-1,4 PB with a molecular weight of 5402 $g.mol^{-1}$. The analysis was carried out by reporting with respect to the temperature, the specific volume, the coefficient of thermal expansion, the total energy, and the constant volume heat capacity averaged over 7 independent configurations. Tait equation was used to fit the evolution of the specific volume for temperatures between 10 K and 700 K and pressure of 0, 60 and 100 MPa.

### Results

The specific volume evolution with temperature and pressure of the melt is predicted to be within 2% of error with the experimental values extrapolated for a similar molecular weight with a very well reproduced coefficient of thermal expansion. The best predictions of Tgs are obtained using the Tait equation fit with a Tg predicted at 162 K at zero pressure and a linear dependence with pressure given a slope of 0.22 K/MPa. As recently observed for PEO and PS, the different calculated properties show hysteresis between the heating and cooling curves.

# Introduction

Polybutadiene (PB) is mainly known as one of the key components employed in tire manufacturing. However, its domain of applicability is relatively wide including coating[1], thermoset additives[2], adhesives[3] and sealing[4]. Consequently, due to its technological importance, the behavior of PB under pressure, and principally its effect on the glass transition temperature (Tg), was extensively studied[5–11]. However, the values of $dT_g/dP$ are relatively dispersed. A such inconsistency can be explained both by the diversity of microstructures encountered in PB and the diversity of technics used to evaluate the Tg. The dependence of Tg on contents of cis-1,4-, trans-1,4 and 1,2-units in PB have been demonstrated in several studies[12–16]. However, the establishment of a quantitative relationship between the microstructure and evaluated Tg remains challenging[15, 17]. The fact that the microstructures not only modify the properties of the amorphous region but also the crystallinity can explain this difficulty. In addition, for the same microstructure the properties could depend on the distribution of the repeat unit.

Thanks to atomistic simulations, the Tg for amorphous models can be evaluated for oligomers of very well controlled compositions. As example, Sharma et al.[18] evaluated Tg for both cis and trans 1,4-models of PB composed of 32-mers from specific volume versus temperatures curves obtained between 100 K to 300 K at a cooling rate of 10 K/ns for united (UA) and all atoms (AA) forcefield (FF). Over the same range of temperatures and at a cooling rate of 20 K/ns, Dossi et al.[19] studied the effect of microstructure on pentamers and decamers of hydroxyl terminated PB using the Dreiding AA forcefield. However, to our knowledge, even if different studies have been performed under pressure[20–26], none of them treated of the effect of pressure on Tg. Indeed, Valega Mackenzie et al.[21] studied the mechanical response of copper/polybutadiene joints under stress mixing embedded atom method and Universal AA-FF. Shock-induced structural changes and post-chock relaxations were studied on cis-1,4 polybutadiene melt both using UA-FF [22] and AA-FF forcefield[23]. Hooper et al.[20] used the Tait EOS to fit the PVT data calculated at 298 K for pressure ranging from ambient to 1000 MPa, on a model composed of 40 random copolymer chains composed of 30 units with a microstructure of 40%, 50% and 10% of 1,4-cis, 1,4-trans and 1,2 vinyl units respectively with a UA-FF. They thus concluded that MD simulations reproduce well the experimental properties of interest for energetic materials and explosive applications. On another hand, Tsolou et al. extensively studied the relaxation of cis-1,4-polybutadiene under pressure[24–26] with a UA-FF described in Ref. [24]. They evaluated PVT data, at temperature ranging from 195 K to 430 K and pressure from 0.1 MPa to 300 MPa, for a system composed of 32 chains of cis-1,4 PB of 128 carbon atoms per chain. From the Tait EOS fit they thus derived the thermal expansion coefficient for the melt.

Consequently, in this paper, the PVT data for both the glassy and the melt states of 1,4-cis- PB will be evaluated for temperature ranging from 10 K to 800 K and pressure from ambient to 100 MPa. The isothermal pressure-volume data will be fitted to the Tait equation allowing interpolation at different pressures. The glass transition temperatures dependence on pressure will then be derived from these fits and compared with values obtained by linear and hyperbolic fits. Both PVT data and Tg will be compared with experimental results obtained for similar molecular weight when available.

# Method

In the present work, all calculations were performed within the LAMMPS code[27] integrated into the MedeA computational environment of Materials Design[28]. One hundred configurations of polymer amorphous cells, containing two chains of cis-1,4-Polybutadiene (cPB) with degree of polymerization of 100 (Mn∼5400 g/mol), were generated at 298 K at a density of 0.9 g/cm$^3$. For all simulations the pcff + forcefield was used, which is based on the pcff forcefield[29]. The pcff + forcefield was constructed to work with wide range of polymers[30]. At the second stage, energy minimization was carried out within the NVT ensemble at 100 K during 50 fs with 0.5 fs integration time step. Seven configurations were selected according two criteria based on the gyration radius (Rg) and end-to-end distance (Ree): $\langle R^2ee\rangle/\langle R^2g\rangle = 6$, $\langle R^2ee\rangle/Mn = 0.75$ Å²/(a.u.m.). These configurations were further equilibrated within the following stages: 1) NVT ensemble at 513 K during 100 fs with 1 fs time step and Nose-Hoover

thermostat[31, 32]. 2) NPT ensemble at 513 K and 1 atm. pressure during 10 ns with 0.5 fs time step. For prepared configurations a simulated dilatometry[33] were applied in order to get access to the glass transition temperature. In particular, each cell was relaxed within the NVT ensemble at 800 K during 100 ps with 1 fs time step, then, within the NPT ensemble at 800 K and 1 atm. pressure during 200 ps with 1 fs time step. Then, in two consecutive stages, the system was firstly cooled down from 790 K to 10 K with a 15 K steps during 5300 ps. Then, the reverse protocol was applied to reach 790 K. At each step, an equilibration within NPT ensemble was performed at 1 atm. during 100 ps with a 1 fs time step. The same protocol was then used for P = 60 and 100 MPa.

All the data were averaged over selected configurations, and the specific volume, as well as coefficient of thermal expansion (CTE, α), total energy ($E_{tot}$) and heat capacity ($C_v$) evolution with temperature were plotted at different pressures. Different methods were used to evaluate the dependence of the glass transition temperature (Tg) with the pressure.

Firstly, Tg was evaluated individually for each pressure using hyperbola fit[34]. In the rubbery ($T > T_g$) and glass ($T < T_g$) states, the dependence of the specific volume ($V_{spec}$) is expected to vary linearly with temperature, but at different rates. $T_g$ is then defined as the intersection of the straight lines extracted from the linear fits in these two regimes. These two regimes are separated by a transition domain whose enlargement depends on the cooling/heating rate. In fact, this domain is clearly larger (~ 150 K) than the experimental one (3–5 K), and thus lead to a significant uncertainty in the determination of $T_g$ as the intercept of the two linear fits. Watts and Bacon[35] suggested the use of hyperbola to give an accurate way to such transition. In this work, the specific volume ($V_{spec}$) was fitted according to the following expression:

$$V = V_0 + \frac{(a+b)(T-T_0)}{2} - \frac{(a-b)\sqrt{(T-T_0)^2+w}}{2}$$ (Eq. 1)

The transition domain between the linear regions is determined by the curvature parameter $w$, whereas $T_0$ and $V_0$ define the center of the hyperbola. The glass transition temperature ($T_g$) is assumed here to be equal to $T_0$.

Secondly, coefficient of thermal expansion (CTE, $\alpha = \frac{1}{V}\frac{\partial V}{\partial T}\Big|_P$ Equation 2) and heat capacity ( $C_v = \frac{\partial E_{tot}}{\partial T}\Big|_P$ Equation 3) evolution with temperatures were fitted with a sigmoid function and Tg was assumed as the point in the middle of the sigmoid.

Finally all $V_{spec}\,(T,P)$ data were fitted with Tait equations for amorphous polymer expressed as[36, 37]:

$$V_{spec,g,r}\,(T,P) = V_{0,g,r}\,(T)\left[1 - 0.0894 ln\left(1 + \frac{P}{B_{g,r}(T)}\right)\right]$$ (Eq. 4)

Where:

$$V_{0,g,r}(T) = b_{1g,r} + b_{2g,r}(T - b_5)$$

$$B_{g,r}(T) = b_{3g,r} exp\left(-b_{4g,r}(T - b_5)\right)$$

*g* and *r* being for T < Tg and T > Tg region respectively. The nine parameters were fitted to the values of specific volume ($V_{spec}$) averaged for each temperature and pressures on the two thermal cycles and the seven configurations. The temperature ranges used for the fit were from 10 to 140 K and from 400 K to 700 K for the glassy T < Tg and rubbery T > Tg regions respectively. Tg was evaluated as the intersection between the two Tait equations.

# Results and discussion

Evolution of calculated density with temperature was firstly compared with experimental data for the melt over temperature range from 300 K to 475 K, Fig. 1. In the melt, experimental sample and numerical model are in the same state and results depend slightly of the cooling/heating rate. Consequently, data are directly comparable. Calculated values are averaged over the configurations and the cooling/heating cycles.

Experimental data are explicitly given in Ref.[38] for Mn = 1000 and 3000 $g.mol^{-1}$, so to compare with our data at Mn = 5402 $g.mol^{-1}$ a linear fit, based on extrapolation of experimental data, was performed. Linear fit is well suited to model experimental data as shown by values of $R^2$ presented in Table 1.

Table 1
Parameters of $V_{spec}$ = aT + b fit from experimental data[38] with (*) extrapolation and calculated(**) for Mn = 5402 $g.mol^{-1}$

| Mn ($g.mol^{-1}$) | a ($10^{-4}$ $cm^3.g^{-1}.K^{-1}$) | b ($cm^3.g^{-1}$) | $R^2$ |
|---|---|---|---|
| | *0 MPa* | | |
| 1000 | 9.05 | 0.882 | 0.9988 |
| 3000 | 8.34 | 0.880 | 0.9985 |
| 5402* | 7.50 | 0.876 | |
| 5402** | 8.00 | 0.869 | 0.999 |
| | *60 MPa* | | |
| 1000 | 6.60 | 0.924 | 0.9999 |
| 3000 | 6.25 | 0.913 | 0.9985 |
| 5402* | 5.82 | 0.90 | |
| 5402** | 6 | 0.897 | 0.9996 |
| | *100 MPa* | | |
| 1000 | 5.74 | 0.933 | 0.9999 |
| 3000 | 5.49 | 0.920 | 0.9999 |
| 5402* | 5.20 | 0.903 | |
| 5402** | 6 | 0.905 | 0.9986 |

To get parameters at Mn = 5402 $g.mol^{-1}$ a linear dependence of *a* and *b* parameters with Mn was used at first approximation. Independently of the pressure, calculated data overestimate of less than 2% these extrapolated data providing a current precision as expected for a good atomic forcefield.

Among the different methods employed to evaluate the glass transition temperature, hyperbolic or linear fit of the specific volume ($V_{spec}$) vs. temperature curve is the most commonly used. The evolutions of the specific volume averaged over the cooling or heating cycles and configurations with temperature are provided as a function of the temperature between 10 K and 600 K for three different pressures 0 MPa, 60 MPa and 100 MPa in Fig. 2.

As expected, specific volume follows linear evolutions with temperature within two domains at low and high temperatures. Over both these temperature regions, the values of the specific volume extracted from the cooling and the reheating processes differ by less than 0.0025 $cm^3.g^{-1}$ as visible on the right axis. At

low temperature, cooling and heating data start to diverge to reach a maximum. At high temperature, statistic noise is more important, but data seems also to converge. Similar peaks were observed for models of PS and PEO using united-atom TraPPE forcefield[39]. A such behavior validate the expectations on transition zone predicted by Moynihan[40, 41] after the analysis of experimental observations performed on inorganic glasses. The peaks seem to shift towards higher temperatures with the increase of pressure, see Fig S.I. 1 for a better visualization. However, the statistic noise is too important to apport a definitive conclusion about the position of the maximum of the peaks. Nevertheless, from these curves it's clear that the transition zone spread over ∼220 K from ∼140 K to ∼360 K.

Hyperbolic initial and fit parameters are presented in Table S.I. 1. Strangely the curvature parameters are quite smaller ranging from 0 K to 111 K than 220 K discussed above. In addition, the trend of Tg with pressure is different than expected since calculated Tg decrease with an augmentation of the pressure. This behavior is observed both for cooling and heating cycle.

Coefficient of thermal expansion evolution with temperature was presented in. Figure 3.

Sigmoidal functions were fitted to the raw data to smooth the statistical noise. Hysteresis loops are present for all pressures. As expected, during the transition the CTE values obtained during the re-heating are lower than those obtained during the cooling. The values of CTE calculated for the melt are in good agreement with the experimental data measured for cis-PB Mn = 3000 $g.mol^{-1}$in Ref. [38]. The values of Tg evaluated from these curves are assessed to be given by the temperature in the middle of the sigmoid and are given for cooling (α_C) and heating (α_H) in the equations present in Fig. 3. Here again no clear dependence of Tg with pressure can be extract from these data.

Similar analysis can also be performed on energetic properties as shown by Soldera[42]. The total energies evaluated during the thermal cycles are displayed in Fig. 4. In addition, the variation of energy between cooling and heating cycles for a given temperature is also presented on the right axis.

Hysteresis loops are also observed during the thermal cycle and can be clearly identified looking at the variation of energy. As for the specific volume, the data at low and high temperature are independent on the thermal history with variation inferior to 15 $kJ.cell^{-1}$. From 160 K to 420 K the variation is larger, reaching a peak around 279 K. The peaks seem to shift towards higher temperatures with the increase of pressure, see Figure S.I. 2 for a better visualization. However, as for the specific volume, the statistic noise is too important to apport a definitive conclusion about the position of the maximum of the peaks.

Heat capacity evolution with temperature was presented in Fig. 5.

As for CTE, hysteresis loops can also be observed from raw data of $C_v$, with an overshooting appearing during the re-heating as expected [40, 41]. Sigmoidal functions were fitted to raw data. The values of heat capacity converge to 4.73 ± 0.02 $J.g^{-1}.K^{-1}$ and 5.05 ± 0.03 $J.g^{-1}.K^{-1}$ for low and high temperature domain respectively. These values overestimate the experimental values as expected from calculations

performed with all atoms forcefield[43]. However, $\Delta C_v$ = 0.32 $J.g^{-1}.K^{-1}$ calculated at the glass transition agree well with recent value of $\Delta C_p$ = 0.31 $J.g^{-1}.K^{-1}$ measured for amorphous cis-PB[44]. The values of Tg evaluated from these curves are assumed to be given by the temperature in the middle of the sigmoid and are given for cooling (Cv_C) and heating (Cv_H) in the equations present in Fig. 3. Here again no clear dependence of Tg with pressure can be extract from these data.

Figure 6 represents the evolution of the calculated $V_{spec}$ with temperature, at three different pressures (0 MPa, 60 MPa and 100 MPa), and the Tait equation fitting for low and high temperature regimes and interpolation for different pressures (20 MPa, 40 MPa and 80 MPa).

The fit resulted in an AAD% of 0.3% independently of the thermal cycle. The fitted parameters are listed in, Table S.I. 2.

The Tg is then defined as the temperature for which $V_{spec}$(Tait < Tg) = $V_{spec}$ (Tait > Tg) for each pressure[45]. The evolution of Tg thus determined in function of the pressure is given in Fig. 7. In this case Tg follows a linear trend with pressure (Tg (P) = 0.2457xP + 161.9, $R^2$ = 0.965).

# Discussion

Several methods were used in this study to evaluate the glass transition temperature (Tg) of amorphous cis-1,4 PB. Comparison with experimental data measured at ambient pressure is firstly done before discussing the pressure dependence of Tg. When comparison with experimental data is performed several parameters are important to take into account. It's well known that Tg depends on molecular weight, polydispersity, architecture, crystallinity, technic of determination and thermal history. In our case we deal with pure monodisperse, amorphous cis-PB with Mn = 5402 $g.mol^{-1}$ per dilatometry and calorimetry on samples cooled/heated at a rate of 75 $10^9$ $K.s^{-1}$. Bogoslovov et al.[46] fitted a data set of 36 Tg measured for molecular weights spreading over 4 decades with Fox-Flory relations providing Tg(Mn) = 174.4–12.4 / Mn given an expected Tg of 172 K for Mn = 5402 $g.mol^{-1}$. However, the value of Tg(∞) seems high relatively to 164 K measured for 97.5%cis:2%trans:0.5%vinyl and Mn = 139000 g/mol[15]

Cooling/heating rate used in laboratory and atomistic simulation differs of several orders of magnitude. Currently, fast experimental cooling rate means 100 K/s[47] relatively to $10^9$-$10^{12}$ K/s commonly used in atomistic modeling. Consequently, WLF correction, as described by Soldera et Metatla[48], has to be applied to get comparable data. Universal parameters were used for the WLF correction calculation[48].

The different Tg evaluated in this study before (aTg) after (pTg) WLF correction are given in Table 2.

Table 2
Calculated atomistic glass transition temperature (aTg) and predicted (pTg) after WLF correction obtained in this study with different methods in comparison to experimental values expected for cis-PB (Mn = 5402 g.mol$^{-1}$)

| | **Dilatometry** | | **Tait** | | **CTE** | | **Cv** | |
|---|---|---|---|---|---|---|---|---|
| | heating | cooling | heating | cooling | heating | cooling | heating | cooling |
| aTg | 259 | 258 | 274 | 274 | 248 | 228 | 224 | 195 |
| pTg | 146 | 146 | 162 | 162 | 135 | 116 | 111 | 83 |
| Experimental. | 162[15], 172[46] | | | | | | | |

Evaluation of aTg by sigmoidal fitting of CTE and Cv provides the most important variation of Tg depending on the thermal history. That's also the method providing the lowest values of aTg. Averaging over a higher number of configurations should improve the accuracy of the calculated data and thus provide a better fit with more coherent values of aTg. Without surprise, the values of aTg evaluated using the Tait fit are independent of the thermal history. That's due to the fact that only the values outside the transition zone are taking into account for the fitting. In these low and high temperatures regime zone, the values of $V_{spec}$ obtained during cooling/heating are quite close as visible on Fig. 2. It's more surprising that the variation of Tg with thermal history was not caught by dilatometry fitting with hyperbola. All pTg underestimate the experimental Tg. This difference could be explained by different factors both based on the numerical and experimental determination. Firstly, the experimental data set used to get the dependence of Tg with Mn was not consistent with 5 monodisperse and three polydisperse PB with Tg measured with different technics (capacitance changes, calorimetry, Raman scattering and mechanical spectroscopy). Moreover, lower molecular weight polybutadiene contained up to 20% of vinyl group which is known to shift Tg towards higher values[15] and no information about crystallinity was provided. Secondly, in addition to the error due to the numerical fit, WLF prediction could be improved by calculating the parameters specific to cis-PB. Predictions of Tg by atomistic simulation for PB have already been done in the past[49–53]. Characteristics of the simulations and pTg are given in Table S.I. 3. Linear fit of $V_{spec}$ vs T was the method employed to determine the Tg in all these studies with aTg = pTg ranging from 179 K to 228 K, WLF correction was never applied. It's interesting to notice that the temperature used for the bilinear fits ranges from 25 K to 400 K. From this study, it appears that the transition zone spreads from ~100 K to ~400 K. Consequently, the values of $V_{spec}$ in the high temperature regime used in these previous studies were certainly still in the transition zone, where a linear behavior is not expected.

The dependences of the glass transition temperature (Tg) with pressure (P), $dT_g/dP$ evaluated experimentally for different polybutadiene microstructures are listed in Table 3 with our calculated. value.

Table 3
Pressure shift of glass temperature from literature and this work

| Microstructure | Mn (g/mol) | Crystallinity | $dT_g/dP$ (K/MPa) | reference |
|---|---|---|---|---|
| 95% cis-1,4 PB | unknown | unknown | 0.13 | [5] |
| 41%cis:52%trans:7%vinyl | 8000 | unknown | 0.18 | [8] |
| unknown | 9000 | unknown | 0.0798 | [9] |
| unknown | 20000 | unknown | 0.064 | [9] |
| 55% 1,2 PB + 45% 1,4 PB | unknown | unknown | 0.17 | [54] |
| unknown | 8000 | unknown | 0.11 | [55] |
| *100% Cis-1,4 PB* | *5402* | *amorphous* | *0.24* | *This work* |

From these experimental values, a variation of 100 MPa leads to a change of Tg of around 10 K. A so small variation could be difficult to observe with atomistic simulation due to the fast cooling/heating rate commonly used. That's why the pressure dependence of Tg evaluated with classical method (dilatometry, CTE and Cv) is not observed over the pressure range used for this study as visible on Fig. 7. On contrary, using the values of Tg predicted by the Tait equation, the augmentation of Tg with the pressure is well reproduced.

From the experimental extreme values of Tg(1502 g/mol, 0 MPa) and of dTg/dP extracted from the Table 2 and Table 3 respectively, it's possible to calculate a domain presenting the evolution of Tg with pressure. This grey domain limited by the dashed line is visible in Fig. 7. The predicted values are within this domain for pressure below 150 MPa. To improve the prediction at high pressure, new calculations seem to be necessary.

# Conclusion

In this study, the effect of thermal cycling on dilatometric and energetic properties of amorphous cis-1,4 polybutadiene has been investigated using atomistic molecular dynamics with the pcff + forcefield. Evolutions of the specific volume, thermal expansion coefficient, total energy and constant volume heat capacity have been monitored in function of the temperature during the cooling and the heating at constant rate for three different pressures. Hysteresis of relaxation has been observed for all properties and pressures. These descriptors can generally be used to evaluate the glass transition temperature. Better agreement with experimental results was obtained for glass transition temperature evaluated with a hyperbolic fit of dilatometry curves but without reproducing the pressure dependence. Tait equation has been used to fit P-V-T data and correctly predict the pressure dependence of the glass transition temperature. From these different results it appears that this method associated with the pcff + forcefield are able to deal with cis-1,4 polybutadiene. To get a clear idea about the effect of microstructure on properties of polybutadiene, trans-1,4 and vinyl moieties have now to be investigated.

## Declarations

# Acknowledgments

The work of A.Shamsieva and I.Piyanzina has been supported by the Kazan Federal University Strategic Academic Leadership Program (PRIORITY-2030) .

The authors declare that no funds, grants, or other support were received during the preparation of this manuscript.

The authors have no relevant financial or non-financial interests to disclose.

All authors contributed to the study conception and design. Methodology was proposed by B. Minisini and applied by A. Shamseiva and I. Piyanzina. The first draft of the manuscript was written by B. Minisini and all authors commented and improved on previous versions of the manuscript. All authors read and approved the final manuscript.

The datasets generated during and/or analyzed during the current study are available from the corresponding author on reasonable request

# References

1. Li K, Zheng J, Zhi J, Zhang K (2018) Aging constitutive model of hydroxyl-terminated polybutadiene coating in solid rocket motor. Acta Astronautica 151:555–562. https://doi.org/10.1016/j.actaastro.2018.06.060
2. Januszewski R, Dutkiewicz M, Nowicki M, et al (2021) Synthesis and Properties of Epoxy Resin Modified with Novel Reactive Liquid Rubber-Based Systems. Ind Eng Chem Res 60:2178–2186. https://doi.org/10.1021/acs.iecr.0c05781
3. Ludbrook BD (1984) Liquid polybutadiene adhesives. International Journal of Adhesion and Adhesives 4:148–150. https://doi.org/10.1016/0143-7496(84)90021-6
4. Richon GL, Chianese DJ (1985) Elastomeric polybutadiene sealing compound. In: 1985 EIC 17th Electrical/Electronics Insulation Conference. pp 153–156
5. Anderson JE, Davis DD, Slichter WP (1969) Pressure Dependence of Molecular Motion in Some Elastomers. Macromolecules 2:166–169. https://doi.org/10.1021/ma60008a011
6. Sasuga T, Takehisa M (1977) Pressure-volume-temperature behavior of several synthetic rubbers. Journal of Macromolecular Science, Part B 13:215–229. https://doi.org/10.1080/00222347708212203
7. Yi YX, Zoller P (1993) An experimental and theoretical study of the PVT equation of state of butadiene and isoprene elastomers to 200°C and 200 MPa. J Polym Sci B Polym Phys 31:779–788. https://doi.org/10.1002/polb.1993.090310705

8. Frick B, Alba-Simionesco C, Hendricks J, Willner L (1997) Incoherent Inelastic Neutron Scattering on Poly butadiene under Pressure. Progress of Theoretical Physics Supplement 126:213–218. https://doi.org/10.1143/ptp.126.213
9. Cailliaux A, Alba-Simionesco C, Frick B, et al (2003) Local structure and glass transition of polybutadiene up to 4 GPa. Phys Rev E 67:010802. https://doi.org/10.1103/PhysRevE.67.010802
10. Frick B, Alba-Simionesco C, Andersen KH, Willner L (2003) Influence of density and temperature on the microscopic structure and the segmental relaxation of polybutadiene. Phys Rev E 67:051801. https://doi.org/10.1103/PhysRevE.67.051801
11. Frick B, Dosseh G, Cailliaux A, Alba-Simionesco C (2003) Pressure dependence of the segmental relaxation of polybutadiene and polyisobutylene and influence of molecular weight. Chemical Physics 292:311–323. https://doi.org/10.1016/S0301-0104(03)00236-2
12. Colby RH, Fetters LJ, Graessley WW (1987) The melt viscosity-molecular weight relationship for linear polymers. Macromolecules 20:2226–2237. https://doi.org/10.1021/ma00175a030
13. Zorn R, McKenna GB, Willner L, Richter D (1995) Rheological Investigation of Polybutadienes Having Different Microstructures over a Large Temperature Range. Macromolecules 28:8552–8562. https://doi.org/10.1021/ma00129a014
14. Klopffer M-H, Bokobza L, Monnerie L (1998) Effect of vinyl content on the viscoelastic properties of polybutadienes and polyisoprenes — monomeric friction coefficient. Polymer 39:3445–3449. https://doi.org/10.1016/S0032-3861(97)10086-6
15. Makhiyanov N, Temnikova EV (2010) Glass-transition temperature and microstructure of polybutadienes. Polym Sci Ser A 52:1292–1300. https://doi.org/10.1134/S0965545X10120072
16. Kisliuk A, Ding Y, Hwang J, et al (2002) Influence of molecular architecture on fast and segmental dynamics and the glass transition in polybutadiene. J Polym Sci B Polym Phys 40:2431–2439. https://doi.org/10.1002/polb.10295
17. Makhiyanov N, Temnikova EV (2010) Glass Transition, Crystallisation, and Melting Temperatures and the Microstructure of Butadiene Rubbers. International Polymer Science and Technology 37:17–20. https://doi.org/10.1177/0307174X1003700604
18. Sharma P, Roy S, Karimi-Varzaneh HA (2016) Validation of Force Fields of Rubber through Glass-Transition Temperature Calculation by Microsecond Atomic-Scale Molecular Dynamics Simulation. J Phys Chem B 120:1367–1379. https://doi.org/10.1021/acs.jpcb.5b10789
19. Dossi E, Earnshaw J, Ellison L, et al (2021) Understanding and controlling the glass transition of HTPB oligomers. Polym Chem 12:2606–2617. https://doi.org/10.1039/D1PY00233C
20. Hooper JB, Bedrov D, Smith GD, et al (2009) A molecular dynamics simulation study of the pressure-volume-temperature behavior of polymers under high pressure. The Journal of Chemical Physics 130:144904. https://doi.org/10.1063/1.3077868
21. Valega Mackenzie FO, Thijsse BJ (2010) Atomistic simulations of the mechanical response of copper/polybutadiene joints under stress. MRS Online Proceedings Library 1224:1009. https://doi.org/10.1557/PROC-1224-FF10-09

22. He L, Sewell TD, Thompson DL (2013) Molecular dynamics simulations of shock waves in cis-1,4-polybutadiene melts. Journal of Applied Physics 114:163517. https://doi.org/10.1063/1.4824546
23. Lecoutre G, Lemarchand CA, Soulard L, Pineau N (2021) Hugoniostat and Direct Shock Simulations in cis-1,4-Polybutadiene Melts. Macromolecular Theory and Simulations 30:2000068. https://doi.org/10.1002/mats.202000068
24. Tsolou G, Harmandaris VA, Mavrantzas VG (2006) Temperature and Pressure Effects on Local Structure and Chain Packing incis-1,4-Polybutadiene from Detailed Molecular Dynamics Simulations. Macromol Theory Simul 15:381–393. https://doi.org/10.1002/mats.200500088
25. Tsolou G, Harmandaris VA, Mavrantzas VG (2006) Atomistic molecular dynamics simulation of the temperature and pressure dependences of local and terminal relaxations in *cis* – 1,4-polybutadiene. The Journal of Chemical Physics 124:084906. https://doi.org/10.1063/1.2174003
26. Tsolou G, Harmandaris VA, Mavrantzas VG (2008) Molecular dynamics simulation of temperature and pressure effects on the intermediate length scale dynamics and zero shear rate viscosity of cis-1,4-polybutadiene: Rouse mode analysis and dynamic structure factor spectra. Journal of Non-Newtonian Fluid Mechanics 152:184–194. https://doi.org/10.1016/j.jnnfm.2007.10.011
27. Plimpton S, Crozier P, Thompson A (2007) "LAMMPS-Large-scale Atomic/Molecular Massively Parallel Simulator," A Software From Sandia National Laboratories
28. MedeA version 3.5
29. Sun H, Mumby SJ, Maple JR, Hagler AT (2002) Ab Initio Calculations on Small Molecule Analogs of Polycarbonates. In: ACS Publications. https://pubs.acs.org/doi/pdf/10.1021/j100016a022. Accessed 1 Aug 2022
30. Rigby D, Saxe PW, Freeman CM, Leblanc B (2016) Computational Prediction of Mechanical Properties of Glassy Polymer Blends and Thermosets. In: Sano T, Srivatsan TS, Peretti MW (eds) Advanced Composites for Aerospace, Marine, and Land Applications. Springer International Publishing, Cham, pp 157–171
31. Hoover WG (1985) Canonical dynamics: Equilibrium phase-space distributions. Phys Rev A 31:1695–1697. https://doi.org/10.1103/PhysRevA.31.1695
32. Hoover WG (1986) Constant-pressure equations of motion. Phys Rev A 34:2499–2500. https://doi.org/10.1103/PhysRevA.34.2499
33. Rigby D, Roe R (1987) Molecular dynamics simulation of polymer liquid and glass. I. Glass transition. J Chem Phys 87:7285–7292. https://doi.org/10.1063/1.453321
34. Patrone PN, Dienstfrey A, Browning AR, et al (2016) Uncertainty quantification in molecular dynamics studies of the glass transition temperature. Polymer 87:246–259. https://doi.org/10.1016/j.polymer.2016.01.074
35. Watts DG, Bacon DW (1974) Using An Hyperbola as a Transition Model to Fit Two-Regime Straight-Line Data. Technometrics 16:369–373. https://doi.org/10.1080/00401706.1974.10489205
36. Rodgers PA (1993) Pressure–volume–temperature relationships for polymeric liquids: A review of equations of state and their characteristic parameters for 56 polymers. Journal of Applied Polymer

Science 48:1061–1080. https://doi.org/10.1002/app.1993.070480613

37. Padilha Júnior EJ, Soares R de P, Cardozo NSM (2015) Analysis of equations of state for polymers. Polímeros 25:277–288. https://doi.org/10.1590/0104-1428.1621
38. Walsh D, Zoller P (1995) Standard Pressure Volume Temperature Data for Polymers. CRC Press
39. Benoit Minisini, Soldera A (2023) Volumetric and Energetic Properties of Polystyrene and Polyethylene Oxide Affected by Thermal Cycling. Macromol. Theory Simul. 2300008 https://doi.org/10.1002/mats.202300008
40. Moynihan CT (1995) Chap. 1. STRUCTURAL RELAXATION AND THE GLASS TRANSITION. In: Stebbins JF, McMillan PF, Dingwell DB (eds) Structure, Dynamics, and Properties of Silicate Melts. De Gruyter, pp 1–20
41. Moynihan CT, Easteal AJ, Wilder J, Tucker J (1974) Dependence of the glass transition temperature on heating and cooling rate. J Phys Chem 78:2673–2677. https://doi.org/10.1021/j100619a008
42. Soldera A (2002) Energetic analysis of the two PMMA chain tacticities and PMA through molecular dynamics simulations. Polymer 43:4269–4275. https://doi.org/10.1016/S0032-3861(02)00240-9
43. Ungerer P, Nieto-Draghi C, Rousseau B, et al (2007) Molecular simulation of the thermophysical properties of fluids: From understanding toward quantitative predictions. Journal of Molecular Liquids 134:71–89. https://doi.org/10.1016/j.molliq.2006.12.019
44. Wrana C, Schawe JEK (2020) Isothermal crystallization of cis-1.4-polybutadiene at low temperatures. Thermochimica Acta 690:178669. https://doi.org/10.1016/j.tca.2020.178669
45. Grassia L, Carbone MGP, D'Amore A (2011) Modeling of the isobaric and isothermal glass transitions of polystyrene. Journal of Applied Polymer Science 122:3751–3756. https://doi.org/10.1002/app.34789
46. Bogoslovov RB, Hogan TE, Roland CM (2010) Clarifying the Molecular Weight Dependence of the Segmental Dynamics of Polybutadiene. Macromolecules 43:2904–2909. https://doi.org/10.1021/ma9026965
47. R. Forstner, G. W. M. Peters, H. E. H. Meijer (2009) A Novel Dilatometer for PVT Measurements of Polymers at High Cooling – and Shear Rates. Inter Polym Proc 24:114–121. https://doi.org/10.3139/217.2154
48. Soldera A, Metatla N (2006) Glass transition of polymers: Atomistic simulation versus experiments. Phys Rev E 74:061803. https://doi.org/10.1103/PhysRevE.74.061803
49. Okada O, Furuya H (2002) Molecular dynamics simulation of cis-1,4-polybutadiene. 1. Comparison with experimental data for static and dynamic propertiesq. 6
50. Gao Y, Wu Y, Liu J, Zhang L (2017) Effect of chain structure on the glass transition temperature and viscoelastic property of cis-1,4-polybutadiene via molecular simulation. J Polym Sci Part B: Polym Phys 55:1005–1016. https://doi.org/10.1002/polb.24342
51. Saha S, Bhowmick AK (2019) An Insight into molecular structure and properties of flexible amorphous polymers: A molecular dynamics simulation approach. J Appl Polym Sci 136:47457.

https://doi.org/10.1002/app.47457

52. Kang Y, Zhou D, Wu Q, et al (2019) Fully Atomistic Molecular Dynamics Computation of Physico-Mechanical Properties of PB, PS, and SBS. Nanomaterials 9:1088. https://doi.org/10.3390/nano9081088
53. Ebrahimi S, Meunier M, Soldera A (2022) Molecular dynamics simulation of the dynamical mechanical analysis of polybutadiene. Polymer Testing 111:107585. https://doi.org/10.1016/j.polymertesting.2022.107585
54. Huang D, Colucci DM, McKenna GB (2002) Dynamic fragility in polymers: A comparison in isobaric and isochoric conditions. J Chem Phys 116:3925–3934. https://doi.org/10.1063/1.1448287
55. Alba-Simionesco C, Morineau D, Frick B, et al (1998) An analysis of the short and intermediate range order in several organic glass-forming liquids from the static structure factor under pressure. Journal of Non-Crystalline Solids 235–237:367–374. https://doi.org/10.1016/S0022-3093(98)00652-8

## Figures

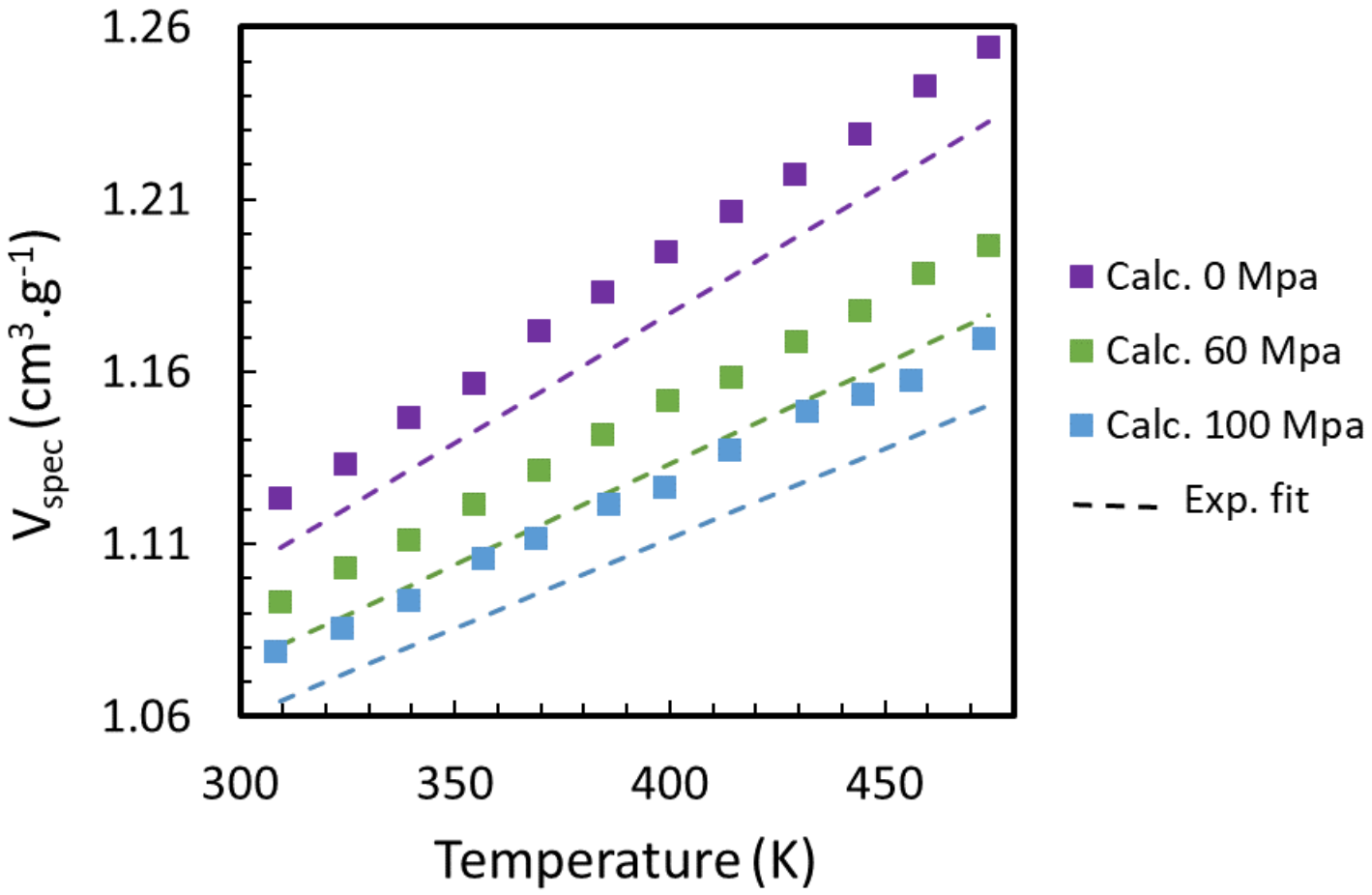


Figure 1

Evolution of the specific volume ($V_{spec}$) as a function of the temperature. Error bars of calculated values are within square symbol. Dashed line, extrapolated from experimental data[38].

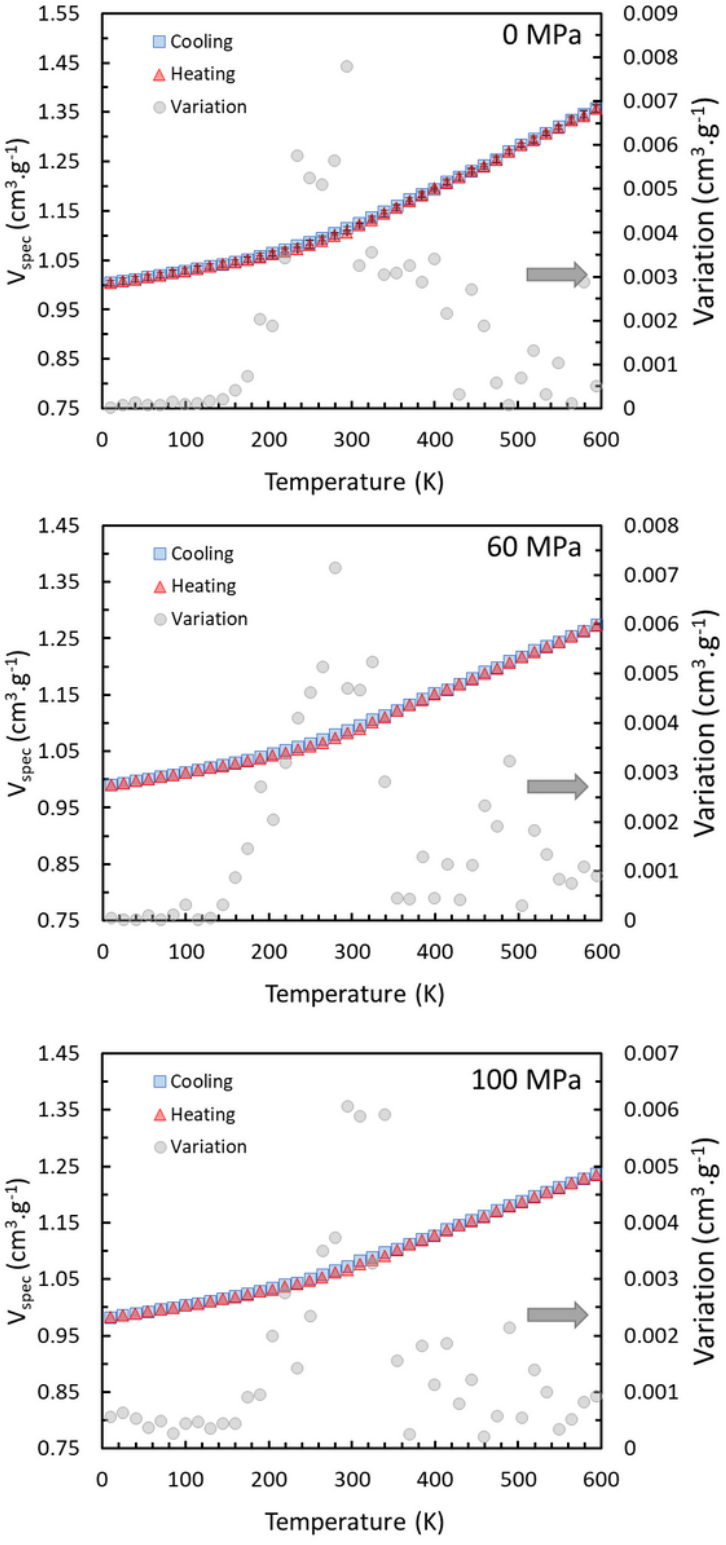


## Figure 2

Evolution of the specific volume as a function of the temperature during the cooling (blue), the heating (red) on the left axis and absolute difference between the specific volume evaluated during the cooling

and the heating on the right axis, for cis-PB model (Mn = 5402 g.mol$^{-1}$).

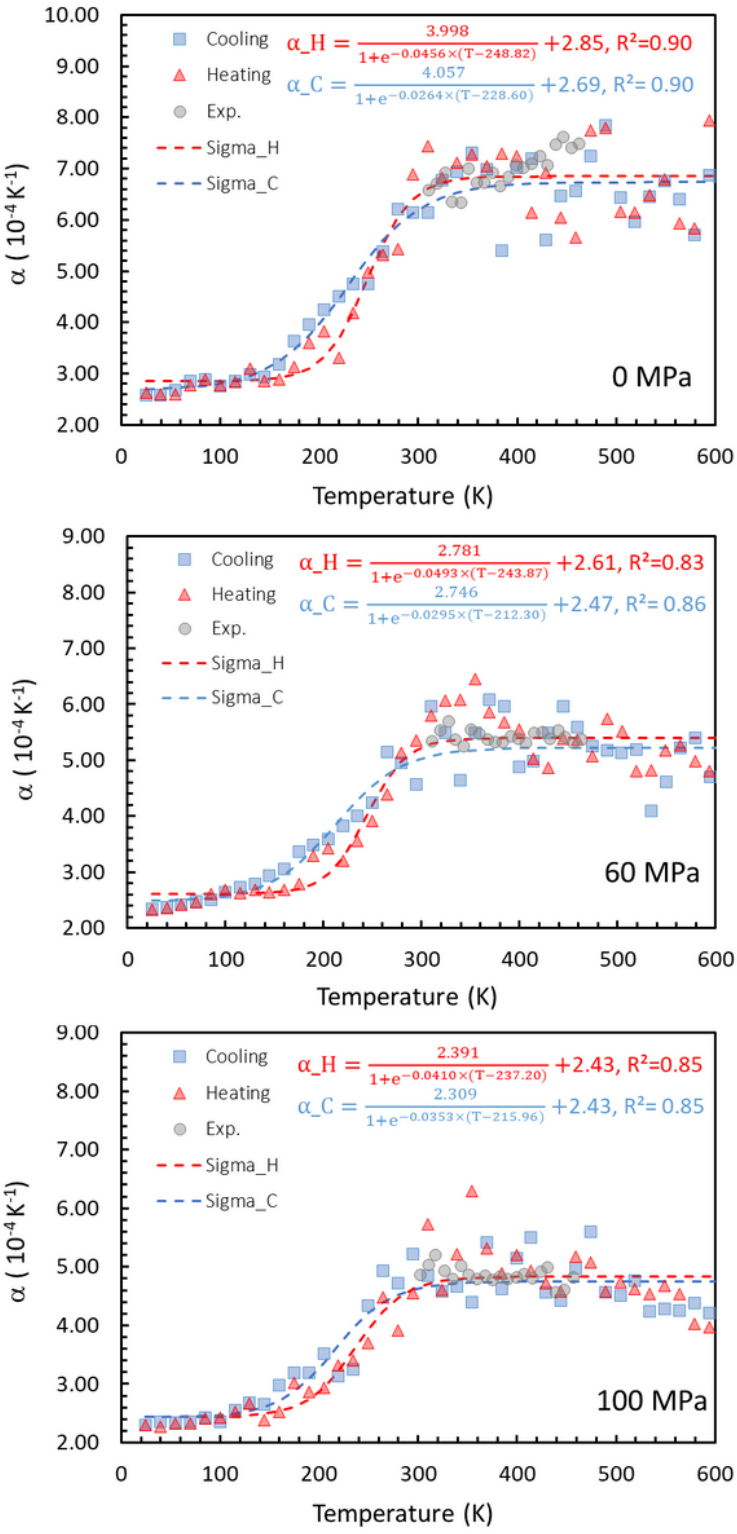


## Figure 3

Coefficient of thermal expansion (a) evolution in respect of temperature for cis-PB Mn = 5200 g.mol$^{-1}$ calculated during cooling/heating cycle. Experimental data are calculated from specific volume given for cis-PB Mn = 3000 g.mol$^{-1}$in [38].

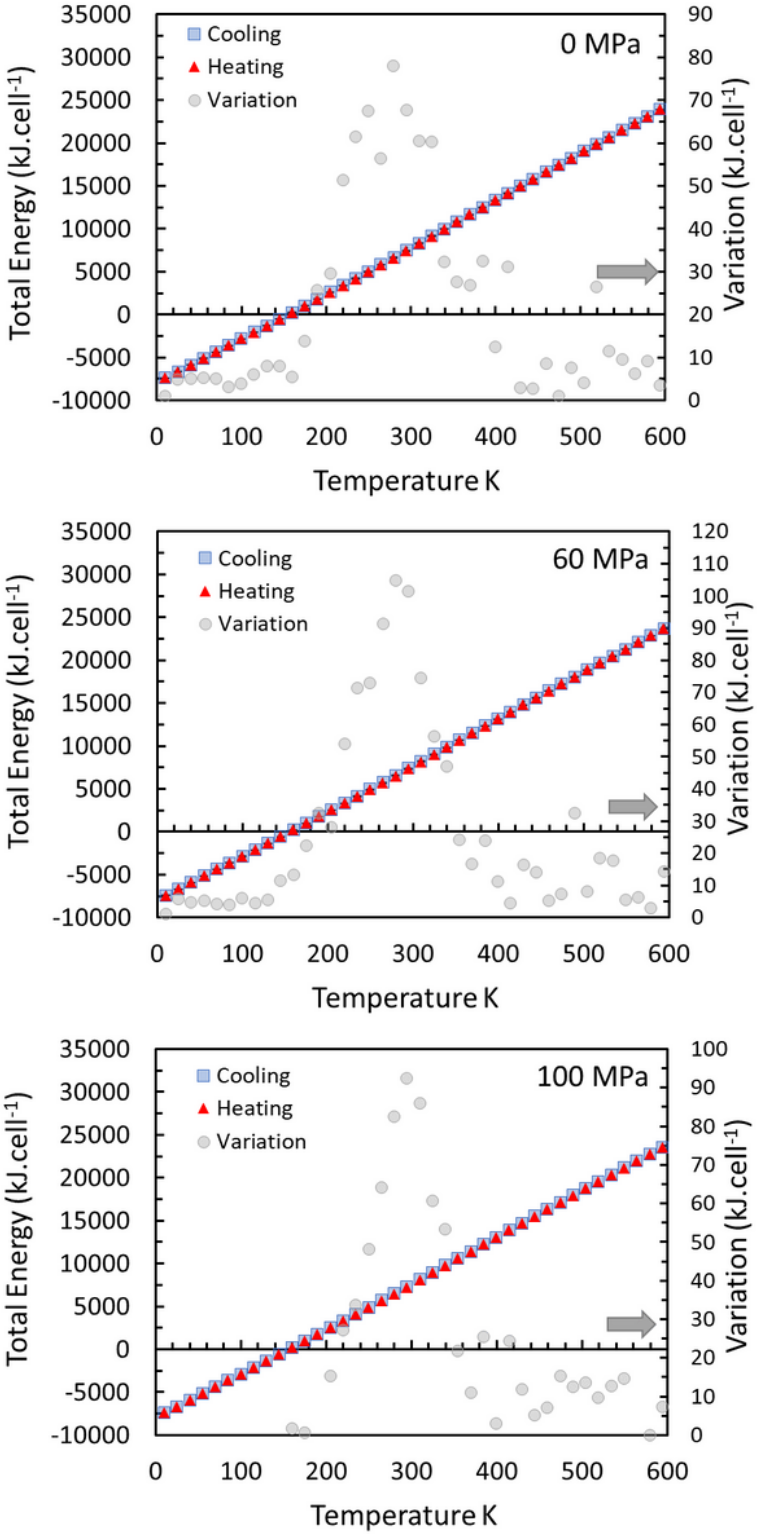


## Figure 4

Evolution of the total energy as a function of the temperature during cooling (blue) and heating (red) on the left axis and difference between the total energy evaluated during the cooling and the heating on the right axis for for cis-PB Mn = 5200 $g.mol^{-1}$.

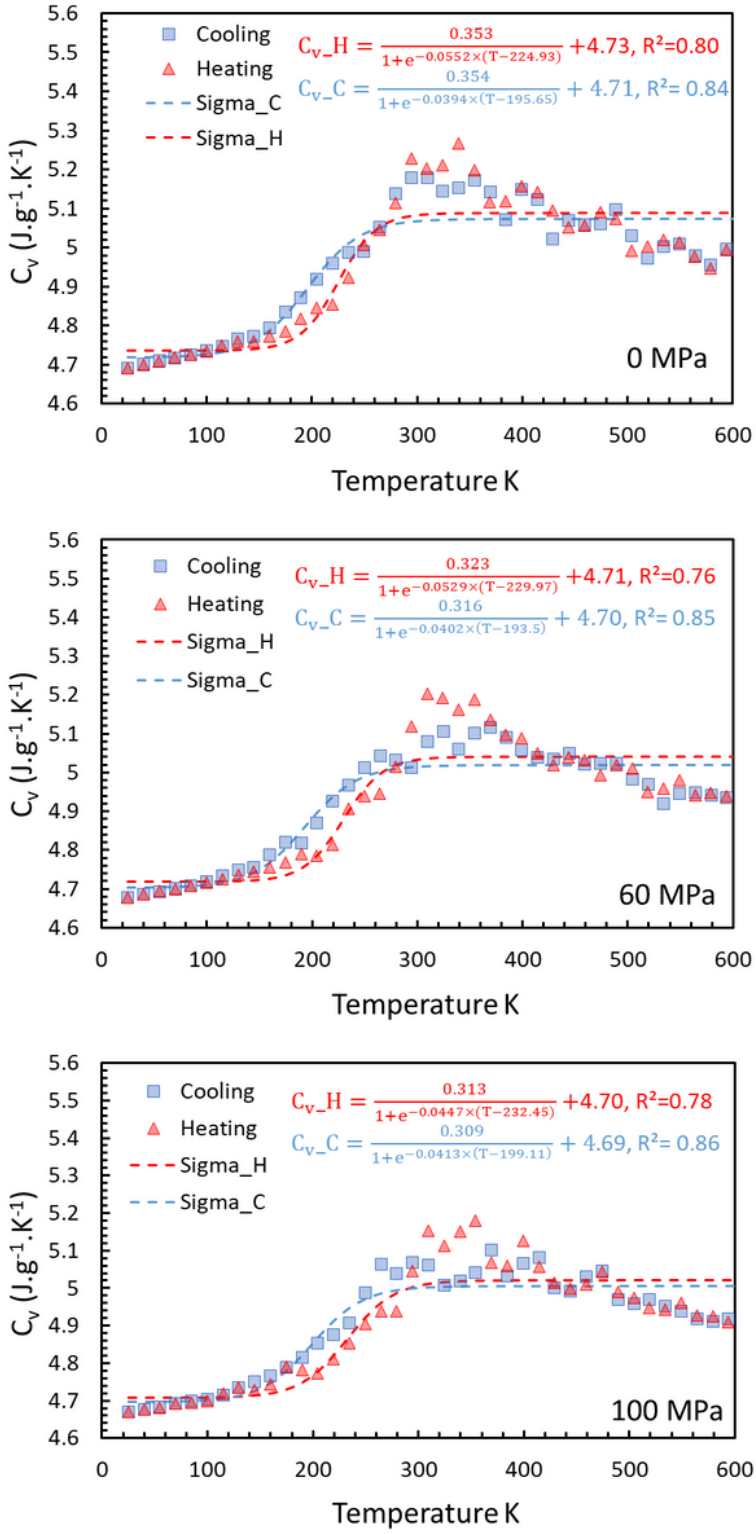


## Figure 5

Heat capacity ($C_v$) evolution in respect of temperature for cis-PB Mn = 5200 g.mol$^{-1}$ calculated during cooling/heating cycle

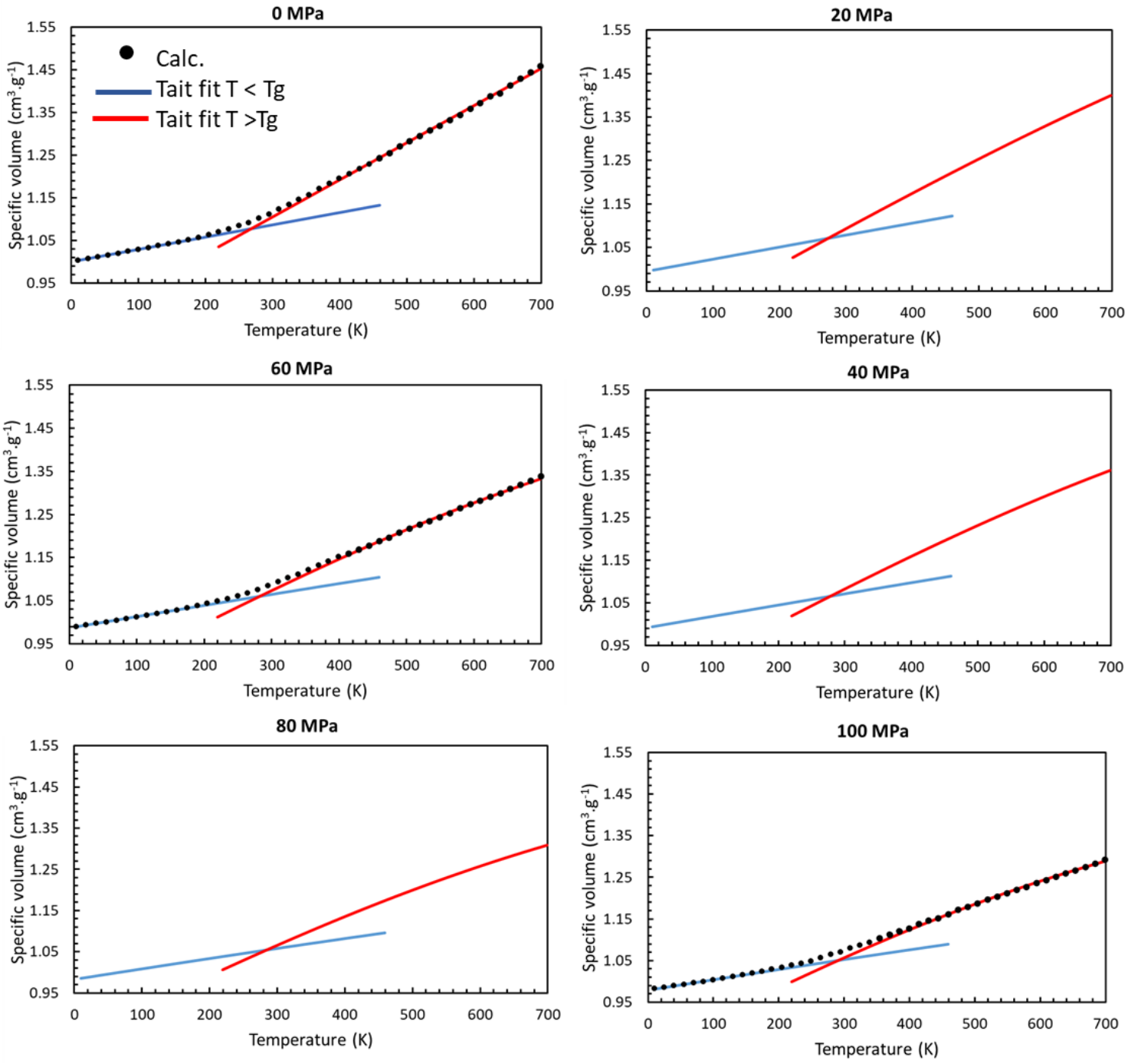


## Figure 6

Specific volume evolution with temperature as calculated at 0, 60 and 100 MPa during heating and Tait's equation fitting at low and high temperature regime.

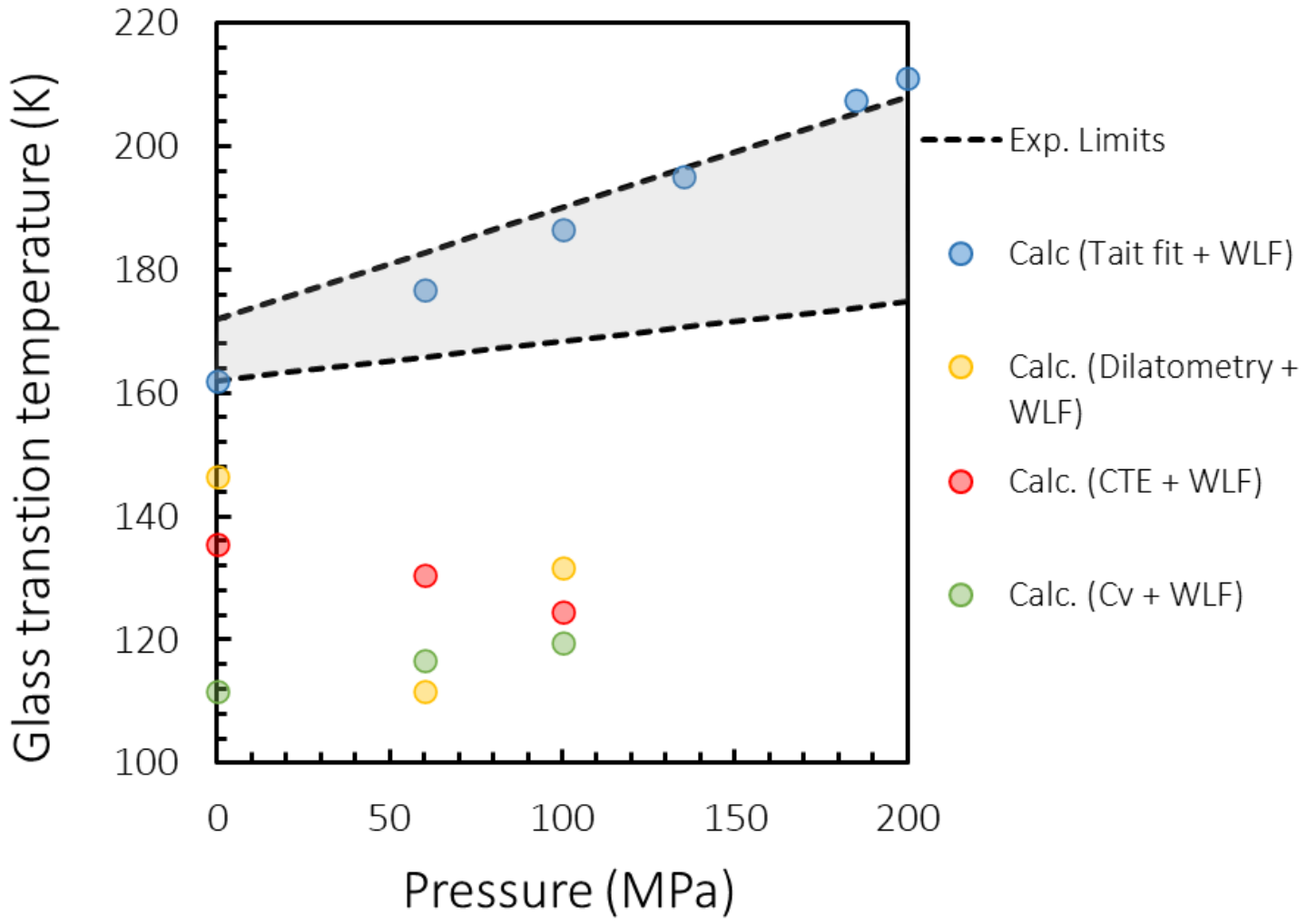


**Figure 7**

Pressure dependence of Tg. Calculated data are given after WLF correction. Exp. limits calculated with Tg(1502 g/mol, 0 MPa)=162 K and $dT_g/dP$ = 0.064 K/ MPa and with Tg(1502 g/mol, 0 MPa)=172 K and $dT_g/dP$ = 0.017 K/MPa

## Supplementary Files

This is a list of supplementary files associated with this preprint. Click to download.

- SI.docx